EG UK Computer Graphics & Visual Computing (2014)
Rita Borgo, Wen Tang (Editors)

Variations on Image Reconstruction: Weighted Back Projection and Fourier Expectation Maximization

A. Ryan[1] and B. Mora[1]

[1]Swansea University Computer Science Department, Swansea, Wales, UK

Abstract

Expectation Maximization and Filtered Back Projection are two common techniques for Tomographic reconstruction of images and volumes. While papers often demonstrat that EM produces higher quality reconstructions, particularly from lower numbers of projections, FBP remains popular due to its low computational complexity. In the following work we present and analyse a modified Expectation Maximization approach which takes advantage of the Fourier Slice Theorem to reduce the bottleneck of forward and back projection. We also investigate Weighted Back Projection, a variation of Filtered Back Projection which uses a weighted average approach to avoid the use of arbitrarily chosen filters.

Categories and Subject Descriptors (according to ACM CCS): I.4.5 [IMAGE PROCESSING AND COMPUTER VISION]: Reconstruction—Transform Methods

1. Introduction

The Expectation Maximization (EM) algorithm is an iterative volume reconstruction method first proposed by Dempster et. al [DLR77] and was later applied to Positron Emission tomography (PET) as an alternative to the Filtered Back Projection (FBP) algorithm by Shepp and Vardi [SV82] due to its ability to better simulate the data acquisition process of PET and being more robust to high levels of sensor noise typical to PET scanning. It is also better suited for scanning methods that use sparse or non-equidistant projection scans. Given the low intensity counts of PET scans, and the long scanning times required, this makes iterative methods such as EM particularly well suited. Recently EM has reveived exposure in other fields in order to produce volumes for Isotropically Emissive Displays (3D display devices) which simulate surfaces and shading [MMCE09].

While EM is shown to produce higher quality reconstructions, Filtered Back Projection (FBP) remains a popular choice in image and volume reconstruction due to its relatively low computation time compared to iterative methods such as EM. In this paper, we also adress a weakness of the FBP method that is the somewhat arbitrary choice of filter function.

In this work we present modifications to the two common reconstruction techniques of FBP and EM. we propose a method for the acceleration of the EM algorithm through the use of Fourier-based forward and back projection in order to remove the computational bottleneck of spatial domain projection and back projection. In doing so we reduce the complexity of the EM algorithm from $O(N^2 \cdot p \cdot i)$ (where N is the number of reconstruction pixels, p is the number of projections and i is the number of iterations), to $(NlogN)$ (the computational complexity of FFT becoming the predominant contributor). While some work has been carried out to investigate the use of Fourier methods for iterative reconstruction techniques [MAK04], no work has explicitly analyzed its application to EM.

We also propose a method to dynamically form a Fourier space filter during the slice insertion step of Fourier reconstruction by the summation of the weights of contribution to each frequency domain pixel during the slice insertion step. This results in a filter direction designed to counteract the overlapping of inserted slices which causes the blurring of back projection. Through this method we reduce the amplitude of the low frequency regions without over amplification of high frequency regions typical to the Ram-Lak filter common in FBP. We also avoid blurring of the resultant reconstruction which can occur when using mid pass filters such as the Hamming window.

DOI: 10.2312/cgvc.20141201

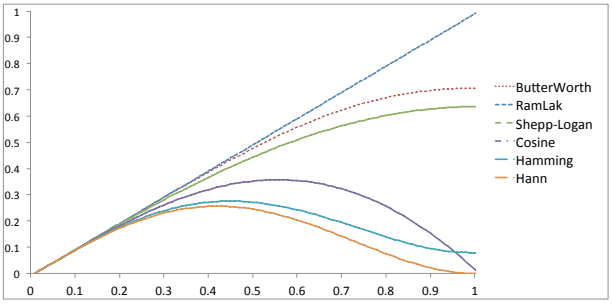

Figure 1: *Shape of frequency domain filters commonly used in FBP*

2. Related Work

2.1. Filtered Back Projection

Filtered Back Projection (FBP) is a common and perhaps the most widely known of the Computed Tomography algorithms, often forming the basis of other derived methods. FBP is typically associated with X-Ray tomography, where detected data is the attenuation of X-Rays across the scanned subject. Back projection is the process of tracing the beam path back through the projection space, setting each sample point to that of the projection data. Repeating for each projection angle the image function $f(x,y)$ is equal to the sum of intensities of all projection pixels $p(\theta,s)$ where θ is the projection angle and s is the distance of the beam perpendicular to θ to the image origin which intersects pixel (x,y).

Back projection alone results in a blurred reconstruction, so filtering of the input projections, which can be done efficiently in the Fourier domain, is required. Common frequency domain filters are shown in Figure 1. The choice of filter leads to trade-offs in quality depending on the filter choice. High pass filters such as the Ram-Lak filter lead to amplification of noise in the reconstruction, while mid pass filters such as the Hamming and cosine filters lead to blurred images and loss of detail in the resultant reconstruction.

Attempts have been made at formalizing the choice of filter used in FBP. One such paper, [FCC*98], attempts to form such a function based on the signal-to-noise ratio resulting from each filter. It concludes however that their method is inadequate to deal with the variations in projection numbers, count-levels, image resolutions and object shape to form an objective selection of an optimal filter function.

Another consideration in FBP is when to apply the filtering. In [ZG94] the authors investigate whether applying the filtering on the back projected data is as accurate as performing the filtering on the input projection data. They conclude that, due to undesirable zeroing of the DC component (where $F(0,0)$) and a finite filtering array, performing the filtering on the input data is the most desirable approach.

2.2. Fourier Slice Theorem and Fourier Reconstruction

An important property of the Fourier Transform for image reconstruction is the *Fourier Slice Theorem*. This theorem (also called the *projection theorem*) states that the projection at angle θ of a 2D function is equal to the inverse FT of a *slice* taken from the 2D FT of the function at angle θ. Therefore an image can be reconstructed by the inverse 2D FT of the 1D FT of its Radon Transform.

In discretized images the slice insertion/extraction process is made non-trivial due to the non-equidistant polar sampling in the slice insertion/extraction step. In order to obtain data between Cartesian grid points, we are required to use the continuous Fourier transform. This is not easily computable and so research has been applied in the use of interpolation to obtain this data for FFT instead. This is a non-trivial task in the frequency domain, with interpolation leading to errors in the obtained projection. Research in the minimization of these errors has led to the development of *Gridding* and the *Non-Uniform Fast Fourier Transform*.

The Fourier Slice Theorem is also extendable to 3D, where the slices are planes rather than lines. This has led to advancements in volume rendering where the theorem can be used to accelerate the projection algorithm from $O(N^3)$ to $O(N^2 logN)$ [Lev92, Mal93].

2.3. Non-Uniform Fast Fourier Transform

A requirement of FFT algorithms is for data to be sampled at equidistant points. This is necessary to allow for the $O(NlogN)$ complexity as opposed to $O(N^2)$ operations of the Discrete Fourier Transform. This results in a problem for radially sampled techniques such as Fourier projection and back projection, where data is sampled on non-equidistant polar samples. In order to still make use of efficient FFT for non-equidistant data, the Non-Uniform Fast Fourier Transform (NUFFT) was proposed by Dutt and Rolkin [Dut95] and later expanded on in [Liu98, FS03]. The NUFFT, which is closely related to gridding algorithms such as that presented in [O'S85], aims to perform an accurate 2D FFT on the polar sampled data by performing interpolation with windowing functions which are highly localized in the frequency domain. We then obtain an approximation on the sampled data by weighting by these scaled window functions. The first step of the NUFFT is a scaling step to pre-compensate for imperfections brought about by the frequency domain interpolation [FCC*98]. [O'S85] And [FS03] both present scaling factors for the pre-computation step. In [FS03] the authors propose a min-max approach to optimise the interpolation coefficients to minimize the worst case error of the reconstruction. They also compare their

approach to the two conventional interpolation functions, namely the Gaussian bell and the Kaiser-Bessel Window.

$$w_j = \begin{cases} \frac{I_0(\pi\alpha\sqrt{1-(2j/J-1)^2}}{I_0(\pi\alpha)} & \text{if } 0 \leq j < J \\ 0 & \text{if otherwise} \end{cases} \quad (1)$$

Equation 1 shows the Modified Kaiser-Bessel (KB) window, where I_0 is the Modified Bessel Function of the first kind of order 0, J is the window width, and α is an arbitrary real number > 0 used to determine the shape of the KB window. In [FS03] the author also uses the min-max approach to optimize the parameters of the Kaiser-Bessel Window. In order to reduce interpolation induced errors an over sampling factor of $K/N = 2$ is used. While it is preferable to use as large an interpolation window as possible, the authors show that $J = 6$ is an adequate trade-off between computational complexity and reconstruction quality. It is shown that $\alpha = 2.34J$ provides the best worst case minimum error [FS03], and so this is the value we have used in our tests.

2.4. Expectation Maximization

EM is an iterative reconstruction technique first applied to the reconstruction of PET scan images by Shepp and Vardi in [SV82] due to its ability to integrate physical properties of the projection model and its robustness to sparse projection data, noise and low emission counts. Despite this its uptake has been slow while FBP remains a prominent technique due to favourable complexity and computation time. An iteration of EM is defined formally as [SV82]

$$f^{*k+1}(b) = f^{*k}(b) \sum_{d=1}^{D} \frac{n^*(d)p(b,d)}{\sum_{b'=1}^{B} f^{*k}(b')p(b',d)}, \; b = 1,\cdots,B \quad (2)$$

where $f^{*k}(b)$ is the reconstructed intensity of pixel/voxel b after k iterations for all $b = 1,\cdots,B$. $p(b,d)$ is the probability of an emission in pixel b being detected at detector tube d for $d = 1,\cdots,D$ given by a known sparse transition matrix (projection matrix). $n^*(d)$ is the total number of emissions detected by d, thus the projection intensity.

In order to reduce the high numbers of iterations required to produce a high quality reconstruction, the Ordered Subset Expectation Maximization (OSEM) was proposed in [HL94]. In this approach, the input projections are divided into smaller subsets. Each subset is operated on in each iteration, with the result from one subset used as the initialization of the next. This results in a significantly higher convergence rate, though does not reduce the complexity of the algorithm.

Convergence in EM is non-uniform [LTIoTO*99]. That is, low frequency regions converge faster than high frequency. This property is taken advantage of in [PY91] where a multi-grid EM (MGEM) implementation is used to accelerate early convergence.

A number of attempts, discussed in [Joh94], have been proposed to stop the EM reconstruction at its "optimal" point. [RMC12] proposes a method for stopping EM when error in the reconstruction is at its lowest or when quality gain per iteration is outweighed by iteration time by comparing the Root Mean Squared Error (RMSE) of the intermediate projections with the input data. When error-reduction per iteration falls below a given threshold, or RMSE increases from one iteration to the next, the process is stopped. In the case of the multi-grid OSEM approach also proposed in [RMC12] this approach is used to control the progression from one resolution to the next, ensuring no time is wasted at lower resolutions when little or no benefit is achieved.

Other applications of EM have recently been explored in [MMCE09] where the author presents it as a solution to the problem of surface visualization in Isotropically Emissive displays. By using EM to produce a light-field that simulates the eyes perception of the surface, a volume is created that can be viewed with both surfaces and shading.

2.5. Fourier Iterative Methods

Little work appears in the literature with regards to the adaptation of Fourier methods for iterative reconstruction algorithms, and to our knowledge no analysis has been done into Fourier methods and the EM algorithm. A key work in this field is presented by Metaj et. al [MAK04] where the authors present an analysis of QPWLS reconstruction with Fourier-based forward and back projectors taking the optimized Kaiser-Bessel interpolation function previously mentioned from [FS03], carrying out an in depth investigation into resultant error based on KB window shape and window size. In this paper it is mentioned that ordered subset approaches do not benefit from Fourier-based methods. This is due to the number of Fourier transforms for each subset. In FEM for example, 4 FFTs are required per iteration (2 foward, 2 inverse). In the case of ordered subsets, this becomes 4 FFTs per subset. This aditional compute time negates the benifits of using Fourier based methods for large numbers of subsets. The paper also acknowledges that while the Fourier Slice theorem is based on parallel beam projection, it can be extended for application to other acquisition methods such as fan and cone beam scanning.

3. Proposed Methods

3.1. Weighted Fourier Reconstruction

Weighted Back Projection is here proposed as an alternative to FBP. An uncontrolled aspect of FFT is in the arbitrary choice of filtering function. The purpose of filtering is to reduce the effect of overlapping back projections, reducing the prevalence of low frequency regions and over blurring of the

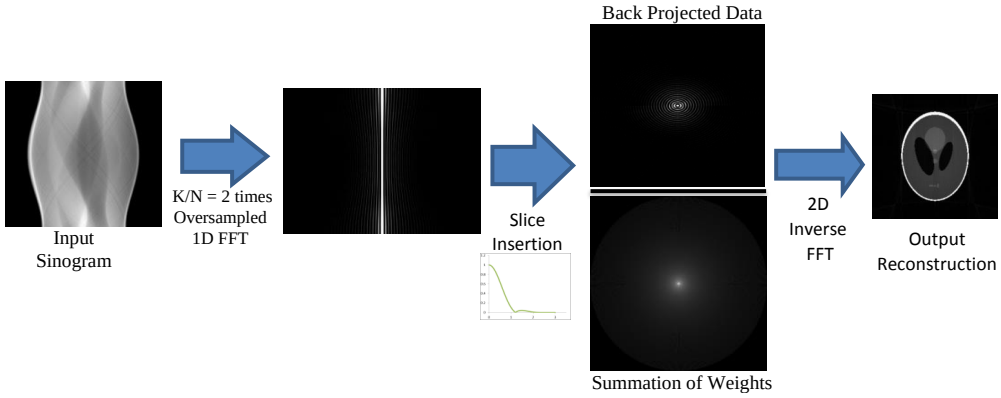

Figure 2: *Weighted Back Projection Process. The input sinogram undergoes super-sampled 1D FFT. The slices of the sinogram FFT are inserted onto a Cartesian grid using $|sinc| * KB$ window interpolation. The sum of interpolation ratios at each pixel is also stored. Inserted slices undergo pixel-wise division by the sum of the interpolation rations. 2D FFT and subsequent unpadding produces our final reconstruction.*

image. In FBP an idealized filter curve such as the Ram-Lak or Shepp-Logan filter is used to approximate the correction curve required to counteract the overlapping of projections.

WBP was inspired by EM where the overlapping of projection data is counteracted by applying weighted averaging to the back projected data as seen by the denominator of the division in Equation 2, the sum of intersections between reconstruction pixel i and projection rays j.

As in FBP, our aim in WBP is to reconstruct the image signal $f(x)$ from input projection sinogram $p(s,\theta)$. Given the input projection sinogram $p(s,\theta)$ and its 1D FFT $\hat{p}(\omega,\theta)$, $\hat{p}$ is typically multiplied with a frequency domain filter $\varphi(\omega,\theta)$ before undergoing inverse 1D FFT and being back projected. Since φ is radially symmetric we define $\varphi(s) = \varphi(s,0)$. The back projection operator $\Re$ is defined formally as

$$(\Re p)(x) = \int_{\theta=0}^{\pi} g(\theta, x\cdot\theta)d\theta \tag{3}$$

Given that p is the projection of function f then this defines back projection as the average of all line integrals over f which intersects pixel x.

Given the filtering function $\varphi(s)$ the filtered back projection function is defined as:

$$(\Re^* p)(x) = \int_{\theta=0}^{\pi} \mathcal{F}^{-1}(\hat{p}(\theta, x\cdot\theta)\varphi(x\cdot\theta))d\theta \tag{4}$$

where $\mathcal{F}^{-1}$ is the inverse Fourier transform and $\hat{p}$ is the 1D Fourier transform of p. In Fourier reconstruction, by the Fourier Slice theorem we have

$$(\Re^* p)(x) = \mathcal{F}^{-1}((2\pi)(\hat{p}(\theta, x\cdot\theta)w(\theta, s\Delta x)d\theta) \tag{5}$$

where for each pixel x in the reconstruction, we take the nearest projection pixel $p(s,\theta)$ where $x\cdot\theta = s$. This is the most basic form of Fourier reconstruction with nearest neighbor back projection. Other methods have used bilinear or cubic interpolation between the nearest cluster of projection pixels, while methods such as Gridding and NUFFT rely on more complex methods.

In Weighted Back Projection, we remove the need for the filtering function φ and replace it with a summation of the interpolated contributions of the slice insertion such that

$$\phi(x) = \sum_{s=-(N-1)/2}^{(N-1)/2} \sum_{\theta=0}^{2\pi} w(\theta, s\Delta x) \tag{6}$$

where w is the chosen interpolation window, and $\theta, s\Delta x, y$ is the distance between points (θ, s) and pixel x after polar to Cartesian coordinate conversion. Since interpolation windows typically have a set width J and are assumed 0 for all distances beyond this, we only calculate w where $\theta, s\Delta x$ is less than $(J-1)/2)$

We therefore define WBP the reconstruction of the estimation f^* of f

$$f^*(x) = \mathcal{F}^{-1}((\Re^* p)(s,\theta)\phi(x)) \tag{7}$$

Previous papers in NUFFT based reconstruction such as [FS03, MAK04] have proposed the use of the Modified Kaiser-Bessel Window (seen in (Figure 3)) as the basis function for the Cartesian-to-polar interpolation . While this produces accurate approximations of the polar sampled Fourier

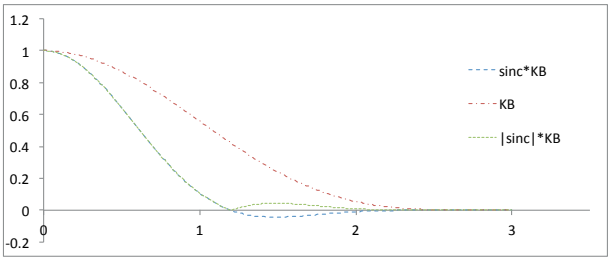

Figure 3: *Interpolation Windows. KB is the Kaiser-Bessel Window where* $J = 6$ *and* $\alpha = 2.34J$

transform a pre-compensation scaling by a windowed *sinc* function is required.

In our practical implementation of WBP we experiment with alternate basis functions shown in Figure 3. In order to satisfy the condition that $\psi(0) = 1$ and $\psi(k) = 0$ where $k \in \mathbb{Z}$ [FS03], we multiply the KB window by the *sinc* function. This maintains a high quality of reconstruction as evident in our results, and does not require pre-compensation. However, we found that at low projection numbers ratio summations were resulting in negative or very low values, resulting in undesirable artifacts due to the weighting step. In trying to maintain reconstruction quality we implemented a $|KB \cdot sinc|$ interpolation kernel. The results of the two approaches are compared in Section 4.

As previously stated in Section 2.1, it has been shown that performing the filtering step on the post-back-projected data results in undesirable zeroing of the Null Frequency and artifacts as a result of the finite extent Fourier Transform [ZG94]. However, our dynamic filter does not cause the undesirable zeroing of the DC component, and we oversample in the frequency domain to counteract the artifacts caused by a finite extent as detailed in many NUFFT based papers [Dut95, FS03, MAK04].

3.2. Fourier Expectation Maximization

A bottleneck in many iterative reconstruction algorithms is the forward and back projections operations. To try and reduce the computation complexity of the EM algorithm we apply a practical application of the Fourier Slice theorem to these stages of the pipeline. We name this process Fourier Expectation Maximization (FEM).

As detailed in NUFFT literature such as [MAK04, FS03], we over sample in the frequency domain by $K/N = 2$ in order to further reduce the artifacts introduced by interpolation. When using Fourier projection and back-projection memory demands of the algorithm increase, as additional buffers of $2N$ and $2P$ elements are required to store the complex frequency domain data as opposed to the real spatial data. This can be reduced by in-line application of the FFT.

During the EM process, the error calculation and reconstruction update steps are pixel-wise multiplications. This would require convolution in the frequency domain. Instead we carry out an inverse FFT to operate in the spatial domain for these steps. Therefore each iteration of the FEM requires two FFTs (before projection and before back projection) and two inverse FFTs (post projection and post back projection).

4. Results

4.1. Implementation and Methodology

In order to test our approaches against the existing methods, four different test cases are used, with the ground truth images shown in Figure 7. A color earth image at 1024^2, a grey-scale version 512^2 Lena, a 256^2 simulated CT slice of the head, and the Shepp-Logan Chest phantom at 256^2. We perform tests using inputs of 32, 64, 128 and 256 projections.

We compare our results to FBP with two different filter choices, the Ram-Lak filter, and the Shepp-Logan filter which can both be seen in Figure 1. We compare the use of $KB \cdot sinc$ and $|KB \cdot sinc|$ interpolation windows in both FBP and WBP. In order to quantitatively assess the performance of each method we compare the Root Mean Squared Error (RMSE) error of the intermediate reconstruction with ground truth images at each iteration and plot against time. We show RMSE results of WBP with both $KB \cdot sinc$ and $|KB \cdot sinc|$ windows, as well as showing results of FBP with both Ram-Lak and Shepp-Logan filters.

Tests are carried out on a single thread on an Intel i7 2.93 GHz. The implementation was developed using C++ and for the implementation of the FFT we use the FFTW 3.0 library

Figure 5: *Input Test cases. Top Left: Earth* 1024×1024*, Top Right: Lena* 512×512*, Bottom Left: CT Head* 256×256*, Bottom RIght: Shepp Logan Chest Phantom* 256×256

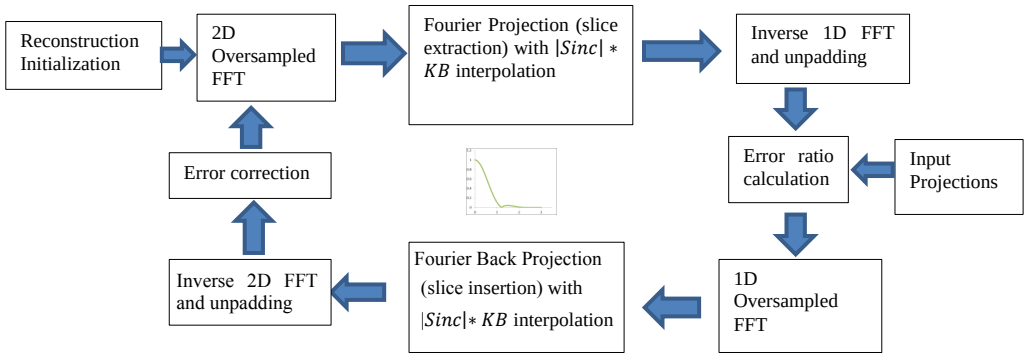

Figure 4: *Fourier EM process. Four oversampled FFTs are required, two forward and two inverse, per update.*

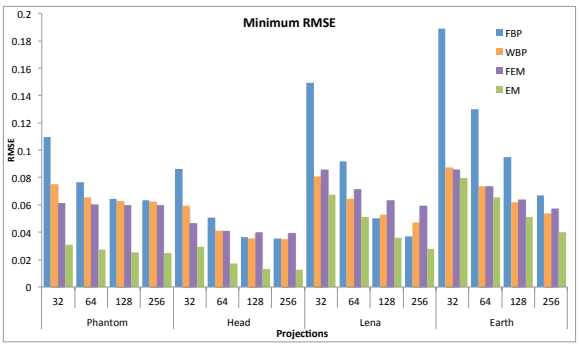

Figure 6: *Minimum achieved RMSE of tested reconstruction techniques for 32, 64, 128 and 256 input projections generated from corresponding ground truths.*

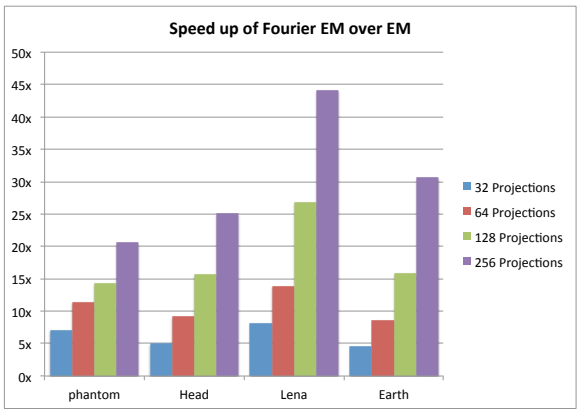

Figure 7: *Multiplicative increase in speed per ieteration between FEM and EM*

4.2. Analysis

Figure 6 shows the minimum RMSE achieved through each reconstruction method tested for the various test cases and input sizes used. The improvements in RMSE between FBP and WBP is most significant when dealing with large datasets with low numbers of input projections. In these cases it is also the case that FEM shows similar benefits over FBP as EM, with the RMSE being substantially lower.

Figure 7 shows the speed-up per iteration of FEM over EM. Figure 6 shows that minimum RMSE is lower for EM reconstructions, the speed per iteration should be considered in the comparison of results. Even with low numbers of projections (32), we observe at least a 5x speed-up per iteration. This speed-up is even greater for larger datasets and a greater number of input projections.

A visual comparison of results can be found in Figures 9, 10, 11 and 12 of the supplementary material. These figures provide a visual comparison of a number of test cases performed. The top two images in each Figure show the best case reconstructions for FBP and WBP on the left and right respectively. That is, the Shepp-Logan filter with filtered back projection, and the $|KB \cdot sinc|$ interpolation method for WBP. It can be seen in all demonstrated test cases that streaking artifacts are significantly reduced through the use of WBP, without introducing significant blurring of the resultant image typical to filters such as the Hamming window in FBP. Figures 9 and 10 do show blurring, however this is due to the low numbers of projections demonstrated in these test cases, a weakness inherent to many transform method reconstructions such as this.

The extent of artifact reduction is demonstrated in Figure 8. Here the reconstruction is shown with a high number of projections (256) with a close up view at a highly contrasting area of the image. A significant reduction in streaking artifacts can be observed in the case of WBP, while the edge of the earth and cloud formations retain clarity and detail.

The bottom two images in each figure represent the recon-

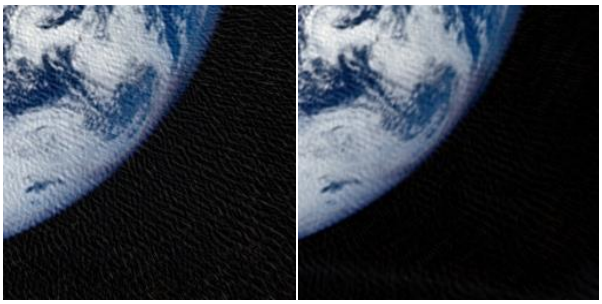

Figure 8: *Close up view of Earth reconstruction, left: FBP with Shepp-Logan Filtering, right: WBP*

struction result representing the lowest RMSE error during the EM and FEM tests. In the case of EM, tests were run for 500 iterations, though it could be continued indefinitely. In the case of FEM, the lowest RMSE occurs around the 90-100th iteration. Visually we observe little difference in the reconstruction between EM and FEM. There is a slight blurring evident in the image, and a slight loss of contrast. The reason for the upward trend in RMSE beyond this point, is that interpolation in Fourier projection introduces error compared to spatial projection. This means that, even close to the ground truth, FEM will not converge beyond a certain point. This error can be reduced through further improvements in NUFFT and Fourier Space interpolation.

5. Conclusion

In this work, two alternative methods to image reconstruction have been proposed. We apply Fourier-based forward and back-projection to remove the bottleneck of the forward and back projectors in the Expectation Maximization method. We have demonstrated a significant speed-up per iteration through the use of Fourier Based techniques. Due to the complexity of FEM, speed-up will be even greater for large datasets allowing for higher resolution reconstructions. Final RMSE is higher than EM and WBP but is lower than FBP especially at low numbers of input projections.

We also introduce Weighted Back Projection as an alternative to the popular Filtered Back Projection method. We show that by correcting back projected data according to the sum of interpolation weights at each pixel, we are able to produce consistently higher quality reconstructions than FBP with common filter functions. Importantly, the reconstruction quality with WBP is considerably higher at low numbers of input projections where FBP typically provides poor quality reconstruction. WBP removes the streaking artifacts typical to FBP while not resulting in subsequent blurring of the image from the use of mid-pass filters such as the Cosine filter or Hamming Window.

In our application of WBP we investigated the use of the modified Kaiser-Bessel window applied to the *sinc* function. We found that this procedure negates the need for correctional scaling required by NUFFT.

References

[DLR77] DEMPSTER A., LAIRD N., RUBIN D.: Maximum likelihood from incomplete data via the em algorithm. *Journal of the Royal Statistical Society 39*, 1 (1977), 1–38. 1

[Dut95] DUTT V. R. A.: Fast fourier transforms for nonequispaced data, ii. *Applied and Computational Harmonic Analysis 2*, 1 (1995), 85–100. 2, 5

[FCC*98] FARQUHAR T., CHATZIIOANNOU A., CHINN G., DAHLBOM M., HOFFMANN E.: An investigation of filter choice for filtered back-projection reconstrion in pet. *IEEE Transactions on Nuclear Science 45*, 3 (June 1998), 1133. 2

[FS03] FESSLER J. A., SUTTON B. P.: Nonuniform fast fourier transforms using min-max interpolation. *IEEE Transactions on Signal Processing 51*, 2 (February 2003), 560–574. 2, 3, 4, 5

[HL94] HUDSON H. M., LARKIN R. S.: Accelerated image reconstruction using ordered subsets of projection data. *IEEE Transactions on Medical Imaging 13*, 4 (1994), 601–609. 3

[Joh94] JOHNSON V.: A note on stopping rules in em-ml reconstructions of ect images. *Medical Imaging, IEEE Transactions on 13*, 3 (1994), 569–571. 3

[Lev92] LEVOY M.: Volume rendering using the fourier projection-slice theorem. In *Also Stanford University* (1992), pp. 61–69. 2

[Liu98] LIU Q. H.: An accurate algorithm for nonuniform fast fourier transforms (nufft's). *IEEE Microwave and Guided Wave Letters 8*, 1 (January 1998), 18–20. 2

[LTIoTO*99] LIU Z., TOKYO INST. OF TECHNOL. YOKOHAMA J. I. S. . E. L., OBI T., YAMAGUCHI M., OHYAMA N.: An investigation of convergence rates in expectation maximization (em) iterative reconstruction. Nuclear Science Symposium, 1999. Conference Record. 3

[MAK04] MATEJ S., A.FESSLER J., KAZANTSEV I. G.: Iterative tomographic image reconstruction using fourier-based forward and back-projectors. *IEEE Transactions on Medical Imaging 23*, 4 (2004), 401–412. 1, 3, 4, 5

[Mal93] MALZBENDER T.: Fourier volume rendering. *ACM Transactions on Graphics 12* (1993), 233–250. 2

[MMCE09] MORA B., MACIEJEWSKI R., CHEN M., EBERT D. S.: Visualization and computer graphics on iso tropically emissive volumetric displays. *IEEE Transactions on Visualization and Computer Graphics 15*, 2 (2009), 221–233. 1, 3

[O'S85] O'SULLIVAN J. D.: A fast sinc function gridding algorithm for fourier inversion in computer tomography. *IEEE Transactions on Medical Imaging 4*, 4 (December 1985), 200–207. 2

[PY91] PAN T.-S., YAGLE A. E.: Numerical study of multigrid implementations of some iterative image reconstruction algorithms. *IEEE Transactions on Medical Imaging 10*, 4 (1991), 572–588. 3

[RMC12] RYAN A., MORA B., CHEN M.: On the implementation and analysis of expectation maximization algorithms with stopping criterion. Image Processing (ICIP), 2012 19th IEEE International Conference on, IEEE, pp. 2393–2396. 3

[SV82] SHEPP L., VARDI Y.: Maximum likelihood reconstrction for emission tomography. *IEEE Transactions on Medical Imaging MI-1*, 2 (1982), 113–122. 1, 3

[ZG94] ZENG G., GULLBERG G.: Can the backprojection filtering algorithm be as accurate as the filtered backprojection algorithm? In *Nuclear Science Symposium and Medical Imaging Conference, 1994., 1994 IEEE Conference Record* (Oct 1994), vol. 3, pp. 1232–1236 vol.3. 2, 5

6. Appendix

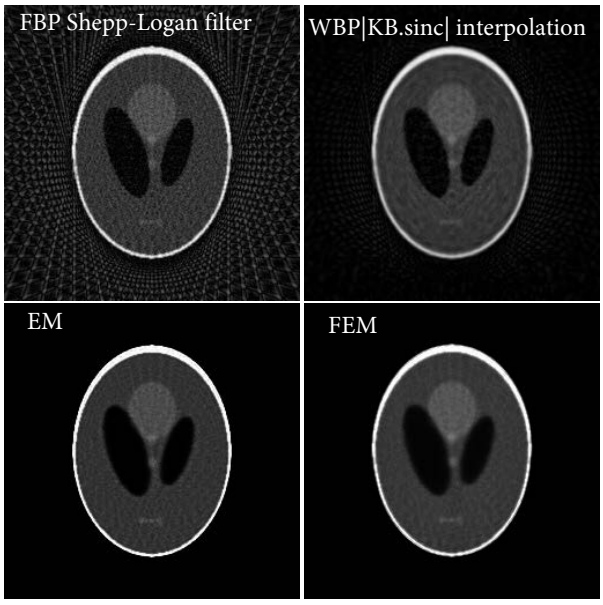

Figure 9: *Phantom Reconstruction Results, 32 projections*

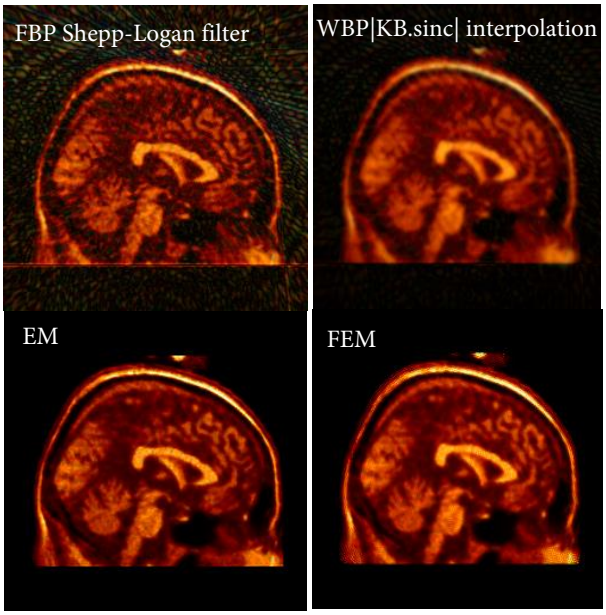

Figure 10: *Head Reconstruction Results, 32 projections*

Figure 11: *Lena Reconstruction Results, 128 projections*

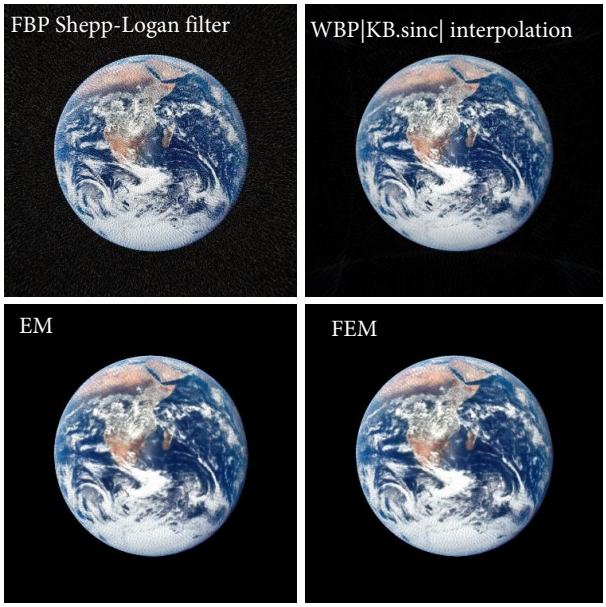

Figure 12: *Earth Reconstruction Results, 256 projections*